Adhesive interactions between milk fat globule membrane and Lactobacillus rhamnosus GG inhibit bacterial attachment to Caco-2 TC7 intestinal cell

Justine Guerin, Claire Soligot, Jennifer Burgain, Marion Huguet, Gregory Francius, Sofiane El-Kirat-Chatel, Faustine Gomand, Sarah Lebeer, Yves Le Roux, Frédéric Borges, et al.

Adhesive interactions between milk fat globule membrane and *Lactobacillus rhamnosus* GG inhibit bacterial attachment to Caco-2 TC7 intestinal cell

Justine Guerin[a], Claire Soligot[b], Jennifer Burgain[a], Marion Huguet[b], Gregory Francius[c], Sofiane El-Kirat-Chatel[c], Faustine Gomand[a], Sarah Lebeer[de], Yves Le Roux[b], Frederic Borges[a], Joël Scher[a], Claire Gaiani[a]

[a]Université de Lorraine, LIBio, F-54000 Nancy, France

[b]Université de Lorraine, URAFPA, Unité de Recherche Animal et Fonctionnalités des Produits Animaux, 2 av de la Forêt de Haye, Vandoeuvre-lès-Nancy, F-54506, France

[c]CNRS, Université de Lorraine, LCPME, Laboratoire de Chimie Physique et Microbiologie pour l'Environnement, UMR 7564, 54600 Villers-lès-Nancy, France

[d]UAntwerpen, Department of Bioscience Engineering, Groenenborgerlaan 171, 2020 Antwerpen, Belgium

[e]Centre of Microbial and Plant Genetics, K.U. Leuven, Leuven, Belgium

*Corresponding author:

claire.gaiani@univ-lorraine.fr

Fax: +33 3 83 59 57 72.

Abstract

Milk is the most popular matrix for the delivery of lactic acid bacteria, but little is known about how milk impacts bacterial functionality. Here, the adhesion mechanisms of *Lactobacillus rhamnosus* GG (LGG) surface mutants to a milk component, the milk fat globule membrane (MFGM), were compared using atomic force microscopy (AFM). AFM results revealed the key adhesive role of the LGG SpaCBA pilus in relation to MFGM. A LGG mutant without exopolysaccharides but with highly exposed pili improved the number of adhesive events between LGG and MFGM compared to LGG wild type (WT). In contrast, the number of adhesive events decreased significantly for a LGG mutant without SpaCBA pili. Moreover, the presence of MFGM in the dairy matrix was found to decrease significantly the bacterial attachment ability to Caco-2 TC7 cells. This work thus demonstrated a possible competition between LGG adhesion to MFGM and to epithelial intestinal cells. This competition could negatively impact the adhesion capacity of LGG to intestinal cells *in vivo*, but requires further substantiation.

Keywords

Lactobacillus rhamnosus GG; Milk fat globule membrane; pili; Atomic force microscopy; Cellular adhesion

Introduction

Pili are long and flexible proteinaceous filaments expressed at the surface of many Gram positive and Gram negative bacteria [1]. Recently, pili were imaged at the surface of the model lactic acid bacterium (LAB) *L. rhamnosus* GG (LGG) [2,3]. LGG has two pili gene clusters in its genome, known as the *spaFED* and *spaCBA*, encoding two distinct kinds of pili: SpaFED pili and SpaCBA pili. Only the *spaCBA* gene cluster is actually expressed in standard laboratory growth conditions [3,4]. LGG contains between 10 to 50 SpaCBA pili per cell, each with an approximate length of 1 µm [3,5,6]. The SpaCBA pili is composed of three pilin subunits [3]. SpaA is the major subunit and constitutes the backbone of the pilus. SpaB is mostly found at the base of the pilus, at the anchorage point with the cell wall, and few of them are also found in the pilus backbone. The SpaC subunits are present along the pilus and at the pilus tip [3]. SpaCBA pilus glycosylation was recently demonstrated and it was suggested that the SpaC pilins are the ones carrying glycosylation [7]. SpaCBA pili are key players in promoting LGG adhesion to a variety of human substrates such as human mucus [6], collagen [6] or intestinal epithelial cells [8]. Adhesive and mechanical properties of pili when interacting with extracellular components of host epithelial layers (mucin or collagen) have been investigated using a non-invasive single cell force spectroscopy method [8]. SpaCBA pili adhesive properties are often attributed to the SpaC subunits. Two adhesive mechanisms were recently proposed. The first mechanism involves a molecular zipper featuring low forces with multiple SpaC subunits disposed along the pilus. The second model proposes a nanospring mechanism implying high forces at the tip of the pilus [6]. Recently, the key role of SpaCBA pili in LGG adhesion to Caco-2 intestinal epithelial cells was confirmed within a study involving LGG surface mutants [9]. The exopolysaccharides (EPS) layer of the LGG surface interfered with the SpaCBA pili during the occurrence of the adhesion phenomenon to epithelial

intestinal cells. The use of a LGG mutant without exopolysaccharides but with increasingly exposed pili improved the adhesion of LGG to epithelial intestinal cells compared to the LGG WT strain [9].

Milk and a wide range of fermented milk products are often used in the industry as LAB delivery systems, which are likely to feature health benefits for the host [10]. Bacterial adhesion to epithelial intestinal cells is influenced by the presence of dairy components. Several studies demonstrated the ability of milk components to modulate pathogenic and probiotic bacteria adhesion to epithelial intestinal cells [11,12]. The addition of acid-hydrolyzed milk decreases the adhesion of *Lactobacillus gasseri* R and *Lactobacillus plantarum* S2 to a co-culture of Caco-2 and HT29-MTX cells [11]. The adhesion of *L. gasseri* R is also negatively affected by the addition of UHT-treated milk or rennet caseins. On the contrary, the addition of bovine serum albumin or whey proteins increases the adhesion of both *L. gasseri* R and *L. casei* FMP strains [12]. These studies show that milk components have the ability to modulate the adhesion of probiotic strains to epithelial intestinal cells. The same behavior was observed for pathogenic bacteria. Defatted milk fat globule membrane (MFGM) prevented *E. coli* O157 : H7 infection by inhibiting bacteria attachment to Caco-2 cells [13]. In another study, bovine mucin extracted from the MFGM inhibited the adhesion of enteric pathogens to Caco-2 cells [14,15]. Dairy products may thus influence bacterial attachment to epithelial intestinal cells but to our best knowledge, no mechanism has yet been described to explain this phenomenon. Interactions between bacterial surface molecule and dairy matrices may negatively impact the attachment of bacteria to intestinal cells.

Adhesive interactions between SpaCBA pili and food matrices, including milk components, are yet poorly studied. The MFGM has gained considerable attention due to its nutritional and technological properties [16]. The MFGM is a thin membrane surrounding the milk fat globule.

MFGM is composed of phospholipids, sphingolipids, and membrane-specific proteins, mainly glycoproteins. A recent review describes the potential role of the glycoprotein mucin 1 (MUC1) in the adhesion phenomenon occurring between bacteria and MFGM [17,18]. In fact, many similarities are observed between the bovine MFGM mucin and human intestinal mucin [19,20]. Bacterial adhesive properties in relation to intestinal mucin have already been described [21], whereas surprisingly, the adhesive properties in relation to MFGM have been poorly studied. Microscopic methods were used to decipher the adhesive phenomena occurring between MFGM and bacteria [22–25]. Similarly, the role of MUC1 in adhesion with pathogenic bacteria has already been described [14,15] but the interactive behaviors of MFGM or MUC1 were never studied at the molecular scale.

In this study, a biophysical approach was first implemented to understand how LGG adheres to MFGM using atomic force microscopy (AFM). Then, a biological study was performed to understand how the adhesion of LGG to Caco-2 TC7 intestinal epithelial cells can be modulated by MFGM. For this purpose, LGG surface mutants were employed to decipher how SpaCBA pili influence LGG adhesion to intestinal epithelial cells in the presence or absence of milk components (*i.e.* MFGM).

Materials and Methods

Materials

The wild type strain *L. rhamnosus* GG (ATCC 53103) (LGG WT) and two of its surface mutants were used in this study. The two mutants were the pili-depleted *spaCBA* mutant CMPG5357 (called

LGG *spaCBA* in this study) [9] and the EPS-deficient *welE* mutant CMPG5351 (called LGG *welE*) [26,27].

The isolation of MFGM was adapted from Le *et al.* (2009) with some modifications [28]. For each experimental run, 40 L of raw bovine milk was collected from a stirred cooling tank from a local farm (farm of La Bouzule, Laneuvelotte, France). Milk was first heated at 50 °C to favorize milk creaming. Then, fat globules were separated from skimmed milk using a cream separator (Elecrem1, Elecrem, Fresnes, France). After one night at 4 °C, the cream was churned using a mixer to obtain two fractions: butter and buttermilk. The buttermilk containing the MFGM was added to the final MFGM solution. The butter was melted at 50 °C after adding distilled water (half of the equivalent volume w / w). The total mixture was centrifuged at 3300 *g* for 10 min. The supernatant containing butter oil was eliminated and the butter serum containing the MFGM fraction was rinsed with 20 g of distilled water and was centrifuged at 3300 *g* for 10 min. The suspension of MFGM containing the butter serum was collected and stored in a freezer for one night. The MFGM powder was obtained after freeze-drying the butter serum.

The purified gastric mucin was purchased from Sigma-Aldrich (Mucin from porcine stomach, M1778, France).

The Caco-2 TC7 TC7 cells were obtained from Pr. Yves Leroux (team MRCA, laboratoire URAFPA, Nancy, France).

Atomic force microscopy

Bacteria culture. LGG culture was performed as described by Guerin *et al.* (2016) [29]. Pre-culture of LGG (WT and its surface mutants) was prepared by inoculating 9 ml of fresh MRS broth

with 100 µl of a bacterial stock solution and placed overnight at 37 °C without stirring. This pre-culture was used to inoculate 9 ml of fresh MRS broth and the growth was performed at 37 °C to reach an optical density of 1.2 at 660 nm. Bacteria were centrifuged at 3000 *g* for 10 min and resuspended in 1 ml of phosphate-buffered saline (PBS) buffer (pH 6.8).

Preparation of bacterial surfaces. The bacterial suspension was deposed on a mica coated with a gold layer functionalized with a NH_3 terminated-PEG linker (PT.BORO.PEG.NH3, Novascan, Ames, Iowa, USA) for 15 h at 4 °C (pH 6.8). The mica was rinsed with PBS before use. AFM topographic images confirmed the presence and good coverage of LGG on the mica surface (data not shown).

Preparation of proteins probes. AFM probes with borosilicate glass particles (2 µm) used in this study were purchased from Novascan (PT.BORO.PEG.NH3, Ames, Iowa, USA). These probes were coated with gold and modified with a NH_3 terminated-PEG linker (PT.BORO.PEG.NH3, Novascan, Ames, Iowa, USA). The spring constant of these probes was 0.01 N/m. MFGM or purified mucin were prepared in distilled water at a concentration of 1 % (w/w) and adhered on the probe by immersion at 4°C for 15 h. The time for adsorption was much longer than the time necessary for the proteins to adsorb on the tip. Preliminary experiments confirmed that the tip was covered with proteins (data not shown). Tips were rinsed with milli-Q-grade water before use.

Atomic force microscopy measurement. The bacteria were adhered on a functionalized mica and the AFM probe was brought in contact with the bacterial surface so as to form a molecule-molecule complex governed by intermolecular bonds. When the AFM probe retracts from the substrate surface, the force required for dissociation *i.e.* the unbinding force can be defined as the rupture force occurring when the probe dissociates from the sample (*i.e.* when the interaction bonds break) [30].

Force measurements were performed at room temperature in PBS buffer (pH 6.8) using an Asylum MFP-3D atomic force microscope (Santa Barbara, CA, USA) controlled by the operation software IGOR Pro 6.04 (Wavemetrics, Lake Osewego, OR, USA) as described by Guerin *et al.* (2016) [29]. The cantilever spring constant with borosilicate particle was first determined using the thermal calibration method which provided a value of 0.01 N/m [31]. For each experiment, the force map was recorded on a 10 × 10 µm² surface corresponding to 32 × 32 points, *i.e.* 1024 force curves. AFM force-distance curves were obtained a retraction speed of 400 mm/s.

Curves processing. For each AFM force measurements a force map containing 1024 force curves was recorded. Retraction curves were analyzed to determine the presence of specific adhesive occurrences between bacteria and milk proteins. Specific adhesion revealed the presence of stretching biomolecule signatures on the retraction curve. For each set of experimental conditions, 100 adhesive force curves were selected and the corresponding retractions were analyzed to determine the percentage of adhesive events with specific biomolecules stretching signatures. In this study, the percentage of adhesive events represented are the percentage of specific adhesive phenomena presenting retraction curves which proved to feature specific biomolecules stretching signatures.

Bacterial adhesion to Caco2 TC7 cells

Epithelial cell lines and culture conditions. Epithelial cells Caco-2 TC7 were grown in Dulbecco's modified Eagle's Minimal Essential Medium with 4.5 g/L glucose (DMEM Glutamax, Fisher Scientific) supplemented with 20 % (v/v) of heat-inactivated fetal calf serum (FCS; Gibco®) and 1 % (v/v) of penicillin–streptomycin (5 000 U/ml penicillin and 5,000 µg/ml streptomycin,

Gibco®) and 1 % (v/v) non-essential amino acid ×100 (Gibco®). Cells were conserved in DMEM medium supplemented with FCS and 10 % glycerol in liquid nitrogen.

The Caco-2 TC7 culture was adapted from Kebouchi *et al.* (2016) [32]. Briefly, cells were thawed and seeded in plastic flasks (75 cm^2, Dutscher). After 4 days, cells were trypsinized with 0.05 % of trypsin-EDTA (×1, Gibco®). After 5 min of contact with trypsin, DMEM medium with FCS was added to the culture to inhibit the trypsin action. Cells were recovered after by centrifugation at 1000 rpm for 5 min at 37 °C. The cells pellet was suspended in DMEM (20 % FCS, 1 % antibiotic and 1 % amino acid) and seeded in six well culture plates (Dutscher) at a final concentration of 6 $\times 10^4$ cell per cm^2. Cells were maintained at 37 °C in a humidified atmosphere with 10 % CO_2 and the culture medium was changed every day. The differentiated cell monolayers were obtained after 22 culture days. Two days before the adhesion tests, DMEM without antibiotics was used to avoid bacteria death during the occurrence of the adhesion phenomenon.

LGG cultures conditions. Bacterial stocks were stored at -80 °C in MRS broth with 20 % (v / v) glycerol. Pre-culture of LGG (WT and its surface mutants) were prepared by inoculating 50 ml of MRS broth with 1 ml of bacterial stock and placed at 37 °C for 8 h without stirring. These pre-cultures were used to inoculate 200 ml of fresh MRS broth; bacterial growth was led for 12 h at 37 °C. The cultures were centrifuged at 3000 *g* for 10 min at room temperature. The resulting pellets were washed with HBSS (Hanks' Balanced Salt Solution, Fisher Scientific) to remove the excess of medium and centrifuged at 3000 *g* for 10 min.

To study the role of surface components in the adhesion phenomenon occurring between LGG and Caco-2 TC7, the LGG pellet (WT and its surface mutants) were directly resuspended in DMEM medium supplemented with only 1 % of amino acid (without FCS and antibiotic) at a bacterial concentration around 10^9 CFU/ml.

To study the effect of MFGM addition on LGG adhesion, the bacterial pellets were resuspended in a solution of MFGM (5 mg/ml) in DMEM medium supplemented with only 1 % of amino acid, for 1 h at 37 °C without stirring. The bacteria mixtures were then centrifuged at 500 *g* for 10 min to obtain bacteria cells pellets. The supernatant containing unbound MFGM was removed and the pellets containing bacteria cells were resuspended in DMEM media (1% amino acid) at a concentration around 10^9 CFU/ml.

LGG survival in DMEM. Bacterial viability in cells culture media (DMEM + 1 % amino acids) was determined by comparing the number of LGG initially present in the DMEM with 1 % amino acids solution and the number of LGG in the medium after incubating for 2 h at 37 °C (**Figure S1**). In both cases, solutions containing the bacteria were mixed for 1 min using a vortex homogenizer. Samples were serially diluted in tryptone salt broth and plated on MRS agar. After 48 h incubation at 37 °C, cell counts were performed and expressed using CFU/ml (Colony Forming Units/ml).

MTT toxicity assay. The effects of MFGM on Caco-2 TC7 cell viability was determined through MTT (3-(4,5-dimethylthiazol-2-yl)-2,5-diphenyltetrazolium bromide) toxicity assays. MTT assays involve the reduction of the water soluble MTT, a yellow tetrazolium salt, into a blue formazan dye precipitate, that can be extracted using an organic solvent. The reduction is realized by the mitochondria of metabolically active cells. MTT assays with 22-day Caco-2 TC7 monolayer culture were assessed as described by Bu *et al.* (2016) [33]. Briefly, cells were treated with 4 ml of different MFGM solutions (0.5 and 5 mg/ml in DMEM without FCS and antibiotic) for 2 h at 37 °C. The MFGM solution was then removed and the differentiated Caco-2 TC7 cell monolayers were gently rinsed with 1 ml of HBSS. Cells were then incubated with 3 ml of DMEM (20% FCS, 1 % amino acid and 1 % antibiotic) and 300 µl of MTT solution (5 mg/ml in PBS) for 3.5 h at 37 °C; the medium was then removed and 2 ml of DMSO per well were added. Solutions containing

cells were diluted ten times and transferred on 96-square angled bottom well plates. The plates were covered from light and incubated with orbital shaking (150 rpm) for 10 min. Absorbance was then measured using a microplate reader at a wavelength of 570 nm.

Adhesion tests. Before adhesion, the differentiated Caco-2 TC7 cell monolayers were gently rinsed with 3 ml of HBSS; 4 ml of bacterial suspension (bacteria alone or bacteria incubated with MFGM) were then added to the cells at a concentration of 10^9 CFU/ml to reach a bacteria cells to epithelial cells ratio of 1000:1 [32]. The number of bacteria present in the initial solutions were determined by bacterial enumeration. Bacteria were incubated on epithelial cells during 2 h at 37 °C and the supernatant of each well was removed. The cell monolayers were gently rinsed with HBSS (4 × 1 ml) to obtain non-adherent bacterial suspensions. Caco-2 TC7 cells were then scraped with 3 × 1 ml of Triton® (×100, Sigma) at 0.1 % (v / v). The solution containing Caco-2 TC7 cells with adherent bacteria was passed three times through a needle and then incubated for 30 min at room temperature. Bacterial enumeration was used to evaluate both the number of non-adherent and adherent bacteria in the supernatant. In both cases, the solution containing the bacteria was mixed during 1 min using a vortex homogenizer. Samples were serially diluted in tryptone salt broth and plated on MRS agar. After a 48 h-incubation period at 37 °C, cell counts were determined and expressed using CFU/ml. The number of adherent bacteria per cell was determined using the following equation:

$$\text{Number of adherent bacteria/cell} = \frac{\text{Number of total adherent bacteria } (CFU/ml) \times \text{Triton volume (ml)}}{\text{Number of cells in the well}}$$

Two independent experiment series were performed in triplicate.

Statistical tests.

Experimental data obtained in this study were all analyzed using a one-way analysis of variance (ANOVA) followed by a Tukey's test. Comparisons were performed between LGG WT and the mutant strains. Results were expressed as means ± SEM (Standard Error of the Mean). Differences were considered statistically significant when P value < 0.05. In the figures, means ± SEM followed by a different superscript letter indicate a significant difference ($P<0.05$).

Results and Discussion

Key role of pili in the adhesive interactions occurring between LGG and MFGM.

In the present study, adhesive events between LGG and MFGM were measured using AFM to understand how LGG adheres to MFGM. AFM probes were functionalized with MFGM and bacteria strains were immobilized on mica. The three strains used in this work are LGG wildtype (WT), LGG *spaCBA* mutant [9] (pili-depleted), and LGG *welE* mutant [26,27] (EPS-depleted). Their percentage of adhesive events presenting specific biomolecule stretching signatures with the MFGM probes were 75.5 ± 1.5, 7.0 ± 3.5 and 99.0 ± 1.0 %, respectively (**Figure 1**). The adhesive events of the pili-depleted *spaCBA* mutant were thus drastically decreased in comparison with those occurring for the wild type strain. On the contrary, when SpaCBA pili were overexposed (for the EPS-deficient *welE* mutant), the adhesive events significantly increased compared to the wild type strain. It is known that pili located on the bacterial surface of the LGG *welE* mutant are not embedded anymore within the EPS layer [9], therefore the pili in this mutant are probably fully available to establish contact points with MFGM, explaining the increased number of adhesive

events [34]. These results highlight the key role of SpaCBA pili in the adhesion phenomenon occurring between LGG and MFGM.

To confirm the role of the SpaCBA pilus in the adhesion phenomenon occurring between LGG and MFGM, force profiles of AFM retraction curves were then analyzed for each strain (**Figure 2**). Retraction curves recorded during adhesion between MFGM and LGG WT presented several rupture peaks with a mean number of ruptures of 1.9 ± 0.0, a mean maximal rupture force of 0.5 ± 0.0 nN, and a maximal rupture distance of 5.9 ± 0.1 µm (**Figure 2A**). These signatures are characteristic of stretched biomolecules, which would be present on the bacterial surface [35]. To identify the biomolecule stretched during the adhesion with MFGM, LGG surface mutants were used. The specific signatures recorded for LGG *spaCBA* mutant on retraction curves were rare (7 %) and totally different from those observed with LGG WT (**Figure 2B**), thus confirming a key role of the SpaCBA pili in the adhesion phenomenon occurring between LGG and MFGM. In the absence of pili, the mean number of ruptures was 1.0 ± 0.0, the mean maximal rupture force was 0.1 ± 0.0 nN, and the mean maximal rupture distance was 0.3 ± 0.1 µm. Signatures recorded during biomolecules stretching between the LGG *spaCBA* mutant and MFGM appear similar to saccharide molecules signatures; they could therefore correspond to the EPS [36] stretching behavior , which are more accessible in the absence of pili. In contrast, the specific signatures recorded on the retraction curves for the LGG *welE* mutant contained multiple rupture peaks. The number of rupture peaks and the force parameters increased compared to those recorded for LGG WT. These signatures have a mean number of ruptures of 5.8 ± 0.7, a mean maximal rupture force of 1.2 ± 0.1 nN, and a mean maximal rupture distance of 8.4 ± 1.1 µm. Since the SpaCBA pili are overexposed in the absence of EPS for the LGG *welE* mutant [9], the increase number of adhesion peaks and the increased force may be explained by the better accessibility of the MFGM adhesion sites to the

pili. All these results thus point towards the SpaCBA pilus being the key macromolecule engaged in the adhesion of LGG to MFGM.

The MFGM is composed of many glycoproteins; one of them is a kind of mucin called MUC1. Many similarities in the structure and composition of mucin MUC1 and purified mucin [19,20] have been found. The signatures observed during the retraction of the MFGM-functionalized probe from the LGG *welE* mutant's surface are similar to those observed during the gastrointestinal mucin stretching in another study [37]; this indicates that MUC1 (from MFGM) may be implied in the adhesion phenomenon with LGG. Mucins are highly glycosylated proteins, with multiple lectin-adhesive sites. Gunning *et al*. (2013) explained the multiple adhesion peaks by repeated attachment-detachment cycles of the lectin-functionalized AFM tip present on the mucin chains [37]. These events are achieved with the presence of multiple binding sites along the mucin molecule. During adhesion between MFGM and the LGG *welE* mutant, the relative large number of adhesion peaks observed on the retraction curve may be the result of repeatedly attachment and detachment of mucin MUC1 on the LGG *welE* mutant cells due to the increased number of adhesive sites on pili for this mutant. [37] used the term "glycocode" to talk about signatures with multiple adhesion peaks, typical of glycosylated molecule-stretching as for mucin.

To support our hypothesis concerning the role of mucin MUC1 in the adhesion phenomenon involving MFGM and LGG, forces measurements with purified mucin from porcine stomach were performed using AFM. The adhesive events percentages were 58.5 ± 11.5, 13.0 ± 1.0, and 86.0 ± 2.0 % with LGG WT, LGG *spa*CBA mutant and LGG *welE* mutant, respectively (**Figure 3**). Similar as MFGM, adhesive events decreased for the LGG *spaCBA* mutant compared to LGG WT. On the contrary, adhesive events significantly increased with the LGG *welE* mutant compared to LGG WT. These results suggest a key role for the SpaCBA pilus in LGG adhesion with purified

intestinal mucin. Retraction curves recorded during the occurrence of the adhesion phenomenon between the purified mucin and LGG WT (**Figure 4A**), the LGG *spaCBA* mutant (**Figure 4B**), or the LGG *welE* mutant (**Figure 4C**) confirmed the role of the SpaCBA pilus in adhesion.

The retraction curves recorded for LGG WT presented the specific signatures of stretching biomolecules with a mean number of ruptures of 2.2 ± 0.1, a mean maximal rupture force of 0.8 ± 0.1 nN, and a mean maximal distance of rupture of 0.7 ± 0.0 µm (**Figure 4A**). The similar signatures observed on the retraction curves of LGG WT when interacting with both MFGM or purified mucin (**Figure 5A**) suggest that the mucin MUC1 may be the biomolecule implicated in the adhesion between LGG and MFGM. For the pili-depleted strain, the LGG *spaCBA* mutant, the specific signatures on retraction curves are rare (13.0 %) and totally different from those observed with LGG WT (**Figure 4B**); this indicates that SpaCBA pili are essential for adhesion to occur between purified mucin and LGG. Retraction curves observed between the LGG *welE* mutant and purified mucin contained multiple rupture peaks similar to those observed for MFGM (**Figure 4C**), yet the maximal rupture forces was higher for purified mucin (1.4 ± 0.0 nN of mean value). This could probably due to differences in purity levels; purified mucin is indeed highly purified, whereas MFGM contains milk mucin but also many other biomolecules such as glycolipids and other glycoproteins. Some part of the retraction curves recorded for MFGM and the purified mucin were similar and correspond to the "glycocode" (**Figure 5B**), meaning that the adhesion between LGG SpaCBA pili and MFGM may be governed by the mucin MUC1. The maximal distance of rupture was very important during adhesion between the LGG *welE* mutant and MFGM with a value of 8.4 ± 0.2 µm. The adhesion between the LGG *welE* mutant and purified mucin lead to a maximal distance of rupture of only 1.9 ± 0.2 µm and ruptures observed on retraction curves which returned several times to the baseline. Because MFGM is composed of many different biomolecules, this

could mean that different biomolecules, including MUC1, are successively stretched during the retraction of the MFGM-functionalized AFM probe from the LGG *welE* mutant surface.

SpaCBA pilus play a key role in LGG adhesion to epithelial intestinal cells. A recent study based on the LGG surface mutants suggests that SpaCBA pili play a key role in LGG adhesion to Caco-2 epithelial cells [9]. To validate our culture cells model and confirm the role of bacterial surface components in LGG adhesion to epithelial intestinal cells, the adhesion phenomena occurring between LGG (LGG WT and two of its surface mutants) and Caco-2 TC7 cells was first checked (**Figure 6**).

All results are obtained by counting the number of adhering bacteria per intestinal cell. Our data revealed that the adhesion of LGG to Caco-2 TC7 cells was drastically reduced for the LGG *spaCBA* mutant compared to the WT strain (9.1 ± 1.1 bacteria per cell, *versus* 19.7 ± 3.8, $P < 0.05$). On the contrary, the adhesion capacity of the LGG *welE* mutant to Caco-2 TC7 cells was significantly increased when compared to the WT strain capacity (42.6 ± 4.7 bacteria per cell, *versus* 19.7 ± 3.8, $P < 0.05$). Lebeer *et al.* (2012) demonstrated and explained the improved adhesive capacities of the EPS-deficient *welE* mutant by the increased exposure of the SpaC subunits from the pili SpaCBA [9]. Our results validate the culture cell adhesion experiment and confirm the key role of pilus SpaCBA in LGG adhesion to Caco-2 TC7 epithelial intestinal cells which has been described in the literature [9].

Impact of MFGM on LGG adhesion to Caco 2 TC7 epithelial cells

When comparing proteins-pilus SpaCBA interactions vs. cell-pilus SpaCBA interactions, the stability of proteins during the gastrointestinal digestion is assumed. It was indeed recently demonstrated that some MFGM proteins are resistant to human enzymatic gastrointestinal digestion [38]. Some glycoproteins such as the mucin MUC1, the cluster of differentiation 36, and a significant part of the periodic acid Schiff 6/7 presented a high resistance to proteases thanks to their glycosylation level. Therefore, MFGM has been chosen to study the impact of food matrix composition on bacterial adhesion.

The impact of MFGM addition on LGG adhesion capacity to Caco-2 TC7 epithelial intestinal cells was investigated by comparing the adhesive capacities of LGG in the presence or the absence of MFGM (**Figure 7**), after first validating the nontoxic effect of MFGM on Caco-2 TC7 epithelial intestinal cells viability via a cell integrity MTT assay (**Figure S2**). The key role of the pilus SpaCBA on LGG adhesion to Caco-2 TC7 cells was confirmed by reproducible and repeatable experiments. The number of adherent bacteria per cell was 19.4 ± 2.9, 8.4 ± 0.5 and 29.2 ± 3.1 for LGG WT, the LGG *spaCBA* mutant and the LGG *welE* mutant, respectively. The presence of MFGM drastically decreased the adhesion capacity of LGG WT and the LGG *welE* mutant with a number of adherent bacteria per cell of 8.5 ± 0.2 and 9.0 ± 1.2, respectively. On the contrary, the adhesion capacity of the LGG *spaCBA* mutant was not impacted by the presence of MFGM (8.1 ± 1.6 adherent bacteria per cell).

The presence of MFGM only modified the adhesive capacities of LGG WT and the LGG *welE* mutant. These two strains express SpaCBA pili on their surface. By interacting with pili, MFGM may mask SpaCBA pili adhesion sites to epithelial intestinal cells and thus inhibit the adhesion of LGG WT and the LGG *welE* mutant to Caco-2 TC7 epithelial intestinal cells (**Figure 7**). Additionally, as expected, MFGM does not influence the adhesion to Caco-2 TC7 epithelial

intestinal cells for this mutant, in agreement with the fact that no adhesive events were observed between MFGM and the LGG spaCBA mutant as shown above. The number of adherent bacteria per cell for the wild type strain and the *welE* mutant in the presence of MFGM was similar to the basal level of adherent bacteria per cell expressed for strains without pili. MFGM thus appears to block *SpaCBA* pili adhesion sites to cells but other surface molecules present on LGG WT and the *welE* mutant surfaces still allow adhesive phenomena to occur between WT and *welE* strains and the cells. These molecules are probably the same as those expressed on the *spaCBA* strain surface. Therefore a competition is likely to occur between the dairy matrix and epithelial intestinal cells for the adhesion to LGG SpaCBA pili.

Few studies have compared the efficacy of probiotics in different food matrices and little is known about how the dairy matrix impacts probiotic functionality [39,40]. Dairy products count amongst the most popular matrices used for probiotic delivery because they provide a physiochemical barrier against gastric acid [41]. Milk matrices help bacteria to survive when passing through the stomach thanks to the buffering capacity of milk proteins. Milk proteins are able to create a pH gradient around bacteria permitting a gradual exposure of bacteria to the external low pH leading to an increase in bacterial survival [42,43]. The delivery matrix can also modify the functional traits at the site of delivery in the gut but very few studies look at this aspect. For example, the functionality of *L. casei* BL23 is improved in milk. When *L. casei* BL23 is added in milk, its effect on reducing the development of colitis is improved [44]. The adhesion of LGG to Caco-2 TC7 epithelial intestinal cells is also reinforced after incubation in yogurt vs. ice cream and the binding properties of bacteria are correlated to the product storage time [45]. Our study brought to light new knowledge on how food matrices impact probiotic efficacy. The consumption of LGG with

MFGM may significantly decrease the adhesion of LGG to Caco-2 TC7 cells, possibly lowering the resulting/associated health impacts.

Conclusion

The ability of MFGM to inhibit the attachment of LGG to host cells was demonstrated. By using two complementary approaches (biophysical and biological), a mechanism was proposed to explain how MFGM can impact bacterial adhesion to intestinal epithelial cells (**Figure 8**). The biophysical approach using AFM revealed that LGG is able to interact with MFGM through SpaCBA pili. The biological approach using cellular adhesion highlighted that LGG SpaCBA pili also play a key role in the intestinal epithelial cells adhesion phenomenon. When bacteria integrated within a native dairy matrix (as it is the case for some MFGM glycoproteins) reach the intestine, pili adhesive sites are thus probably blocked by milk proteins such as MFGM and therefore bacterial adhesion to intestinal cells can be inhibited or limited. As many lactic acid bacteria are incorporated into dairy products, much research should be performed in order to check if bacterial functionality is preserved in the presence of dairy components. This knowledge on adhesive mechanisms may also be important when formulating new nutraceutical products when the goal is to inhibit the adhesion of pathogenic bacteria to the intestine.

Supporting Information. The LGG survival in DMEM + 1 % amino acid was determined in Figure S1. The nontoxic effect of MFGM on Caco-2 TC7 epithelial intestinal cells viability was determined via a cell integrity MTT assay (Figure S2).

References

[1] K.A. Kline, S. Falker, S. Dahlberg, S. Normark, B. Henriques-Normark, Bacterial Adhesins in Host-Microbe Interactions, Cell Host Microbe. 5 (2009) 580–592. doi:10.1016/j.chom.2009.05.011.

[2] P. Tripathi, V. Dupres, A. Beaussart, S. Lebeer, I.J.J. Claes, J. Vanderleyden, Y.F. Dufrene, Deciphering the Nanometer-Scale Organization and Assembly of Lactobacillus rhamnosus GG Pili Using Atomic Force Microscopy, Langmuir. 28 (2012) 2211–2216. doi:10.1021/la203834d.

[3] J. Reunanen, I. von Ossowski, A.P. Hendrickx, A. Palva, W.M. de Vos, Characterization of the SpaCBA pilus fibers in the probiotic Lactobacillus rhamnosus GG, Appl Env. Microbiol. 78 (2012) 2337–44. doi:10.1128/aem.07047-11.

[4] F.P. Douillard, A. Ribbera, H.M. Järvinen, R. Kant, T.E. Pietilä, C. Randazzo, L. Paulin, P.K. Laine, C. Caggia, I. von Ossowski, J. Reunanen, R. Satokari, S. Salminen, A. Palva, W.M. de Vos, Comparative Genomic and Functional Analysis of Lactobacillus casei and Lactobacillus rhamnosus Strains Marketed as Probiotics, Appl. Environ. Microbiol. 79 (2013) 1923–1933. doi:10.1128/AEM.03467-12.

[5] M. Kankainen, L. Paulin, S. Tynkkynen, I. von Ossowski, J. Reunanen, P. Partanen, R. Satokari, S. Vesterlund, A.P. Hendrickx, S. Lebeer, S.C. De Keersmaecker, J. Vanderleyden, T. Hamalainen, S. Laukkanen, N. Salovuori, J. Ritari, E. Alatalo, R. Korpela, T. Mattila-Sandholm, A. Lassig, K. Hatakka, K.T. Kinnunen, H. Karjalainen, M. Saxelin, K. Laakso, A. Surakka, A. Palva, T. Salusjarvi, P. Auvinen, W.M. de Vos, Comparative genomic analysis of Lactobacillus rhamnosus GG reveals pili containing a human- mucus binding protein, Proc Natl Acad Sci U A. 106 (2009) 17193–8. doi:10.1073/pnas.0908876106.

[6] P. Tripathi, A. Beaussart, D. Alsteens, V. Dupres, I. Claes, I. von Ossowski, W.M. de Vos, A. Palva, S. Lebeer, J. Vanderleyden, Y.F. Dufrene, Adhesion and Nanomechanics of Pili from the Probiotic Lactobacillus rhamnosus GG, ACS Nano. 7 (2013) 3685–3697. doi:10.1021/nn400705u.

[7] H.L.P. Tytgat, N.H. van Teijlingen, R.M.A. Sullan, F.P. Douillard, P. Rasinkangas, M. Messing, J. Reunanen, R. Satokari, J. Vanderleyden, Y.F. Dufrêne, T.B.H. Geijtenbeek, W.M. de Vos, S. Lebeer, Probiotic Gut Microbiota Isolate Interacts with Dendritic Cells via Glycosylated Heterotrimeric Pili, PloS One. 11 (2016) e0151824. doi:10.1371/journal.pone.0151824.

[8] R.M.A. Sullan, A. Beaussart, P. Tripathi, S. Derclaye, S. El-Kirat-Chatel, J.K. Li, Y.J. Schneider, J. Vanderleyden, S. Lebeer, Y.F. Dufrene, Single-cell force spectroscopy of pili-mediated adhesion, Nanoscale. 6 (2014) 1134–1143. doi:10.1039/c3nr05462d.

[9] S. Lebeer, I. Claes, H.L. Tytgat, T.L. Verhoeven, E. Marien, I. von Ossowski, J. Reunanen, A. Palva, W.M. Vos, S.C. Keersmaecker, J. Vanderleyden, Functional analysis of Lactobacillus rhamnosus GG pili in relation to adhesion and immunomodulatory interactions with intestinal epithelial cells, Appl Env. Microbiol. 78 (2012) 185–93. doi:10.1128/aem.06192-11.

[10] S.S. Dalli, B.K. Uprety, S.K. Rakshit, Industrial Production of Active Probiotics for Food Enrichment, in: Y.H. Roos, Y.D. Livney (Eds.), Eng. Foods Bioact. Stab. Deliv., Springer New York, 2017: pp. 85–118. doi:10.1007/978-1-4939-6595-3_3.

[11] T. Volštátová, J. Havlík, I. Doskočil, M. Geigerová, V. Rada, Effect Of Hydrolyzed Milk On The Adhesion Of Lactobacilli To Intestinal Cells, Sci. Agric. Bohem. 46 (2015) 21–25. doi:10.1515/sab-2015-0012.
[12] T. Volstatova, J. Havlik, M. Potuckova, M. Geigerova, Milk digesta and milk protein fractions influence the adherence of Lactobacillus gasseri R and Lactobacillus casei FMP to human cultured cells, Food Funct. 7 (2016) 3531–3538. doi:10.1039/C6FO00545D.
[13] S.A. Ross, J.A. Lane, M. Kilcoyne, L. Joshi, R.M. Hickey, Defatted bovine milk fat globule membrane inhibits association of enterohaemorrhagic Escherichia coli O157:H7 with human HT-29 cells, Int. Dairy J. 59 (2016) 36–43. doi:10.1016/j.idairyj.2016.03.001.
[14] P. Parker, L. Sando, R. Pearson, K. Kongsuwan, R.L. Tellam, S. Smith, Bovine Muc1 inhibits binding of enteric bacteria to Caco-2 cells, Glycoconj. J. 27 (2009) 89–97. doi:10.1007/s10719-009-9269-2.
[15] L. Sando, R. Pearson, C. Gray, P. Parker, R. Hawken, P.C. Thomson, J.R.S. Meadows, K. Kongsuwan, S. Smith, R.L. Tellam, Bovine Muc1 is a highly polymorphic gene encoding an extensively glycosylated mucin that binds bacteria, J. Dairy Sci. 92 (2009) 5276–5291. doi:10.3168/jds.2009-2216.
[16] K. Dewettinck, R. Rombaut, N. Thienpont, T.T. Le, K. Messens, J. Van Camp, Nutritional and technological aspects of milk fat globule membrane material, Int. Dairy J. 18 (2008) 436–457. doi:10.1016/j.idairyj.2007.10.014.
[17] J. Guerin, J. Burgain, F. Gomand, J. Scher, C. Gaiani, Milk fat globule membrane glycoproteins: Valuable ingredients for lactic acid bacteria encapsulation?, Crit. Rev. Food Sci. Nutr. (2017) 1–13. doi:10.1080/10408398.2017.1386158.
[18] T. Douëllou, M.C. Montel, D. Thevenot Sergentet, Invited review: Anti-adhesive properties of bovine oligosaccharides and bovine milk fat globule membrane-associated glycoconjugates against bacterial food enteropathogens, J. Dairy Sci. 100 (2017) 3348–3359. doi:10.3168/jds.2016-11611.
[19] S. Patton, S.J. Gendler, A.P. Spicer, The epithelial mucin, MUC1, of milk, mammary gland and other tissues, Biochim. Biophys. Acta. 1241 (1995) 407–423.
[20] R. Bansil, B.S. Turner, Mucin structure, aggregation, physiological functions and biomedical applications, Curr. Opin. Colloid Interface Sci. 11 (2006) 164–170. doi:10.1016/j.cocis.2005.11.001.
[21] K. Nishiyama, M. Sugiyama, T. Mukai, Adhesion Properties of Lactic Acid Bacteria on Intestinal Mucin, Microorganisms. 4 (2016). doi:10.3390/microorganisms4030034.
[22] M.H. Tunick, K.L. Mackey, J.J. Shieh, P.W. Smith, P. Cooke, E.L. Malin, Rheology and microstructure of low-fat Mozzarella cheese, Int. Dairy J. 3 (1993) 649–662. doi:10.1016/0958-6946(93)90106-A.
[23] E. Laloy, J.-C. Vuillemard, M. El Soda, R.E. Simard, Influence of the fat content of Cheddar cheese on retention and localization of starters, Int. Dairy J. 6 (1996) 729–740. doi:10.1016/0958-6946(95)00068-2.
[24] C. Lopez, M.-B. Maillard, V. Briard-Bion, B. Camier, J.A. Hannon, Lipolysis during ripening of Emmental cheese considering organization of fat and preferential localization of bacteria, J. Agric. Food Chem. 54 (2006) 5855–5867. doi:10.1021/jf060214l.
[25] C.D. Hickey, J.J. Sheehan, M.G. Wilkinson, M.A.E. Auty, Growth and location of bacterial colonies within dairy foods using microscopy techniques: a review, Food Microbiol. 6 (2015) 99. doi:10.3389/fmicb.2015.00099.
[26] S. Lebeer, I.J.J. Claes, T.L.A. Verhoeven, J. Vanderleyden, S.C.J. De Keersmaecker, Exopolysaccharides of Lactobacillus rhamnosus GG form a protective shield against innate

immune factors in the intestine, Microb. Biotechnol. 4 (2011) 368–374. doi:10.1111/j.1751-7915.2010.00199.x.
[27] S. Lebeer, T.L. Verhoeven, G. Francius, G. Schoofs, I. Lambrichts, Y. Dufrene, J. Vanderleyden, S.C. De Keersmaecker, Identification of a gene cluster for the biosynthesis of a long galactose-rich exopolysaccharide in Lactobacillus rhamnosus GG and functional analysis of the priming glycosyltransferase, Appl Env. Microbiol. 75 (2009) 3554–3563. doi:10.1128/AEM.02919-08.
[28] T.T. Le, J. Van Camp, R. Rombaut, F. van Leeckwyck, K. Dewettinck, Effect of washing conditions on the recovery of milk fat globule membrane proteins during the isolation of milk fat globule membrane from milk, J. Dairy Sci. 92 (2009) 3592–3603. doi:10.3168/jds.2008-2009.
[29] J. Guerin, J. Bacharouche, J. Burgain, S. Lebeer, G. Francius, F. Borges, J. Scher, C. Gaiani, Pili of Lactobacillus rhamnosus GG mediate interaction with β-lactoglobulin, Food Hydrocoll. 58 (2016) 35–41. doi:10.1016/j.foodhyd.2016.02.016.
[30] C.-K. Lee, Y.-M. Wang, L.-S. Huang, S. Lin, Atomic force microscopy: Determination of unbinding force, off rate and energy barrier for protein–ligand interaction, Micron. 38 (2007) 446–461. doi:10.1016/j.micron.2006.06.014.
[31] R. Lévy, M. Maaloum, Measuring the spring constant of atomic force microscope cantilevers: thermal fluctuations and other methods, Nanotechnology. 13 (2002) 33–37.
[32] M. Kebouchi, W. Galia, M. Genay, C. Soligot, X. Lecomte, A.A. Awussi, C. Perrin, E. Roux, A. Dary-Mourot, Y. Le Roux, Implication of sortase-dependent proteins of Streptococcus thermophilus in adhesion to human intestinal epithelial cell lines and bile salt tolerance, Appl. Microbiol. Biotechnol. 100 (2016) 3667–3679. doi:10.1007/s00253-016-7322-1.
[33] P. Bu, S. Narayanan, D. Dalrymple, X. Cheng, A.T.M. Serajuddin, Cytotoxicity assessment of lipid-based self-emulsifying drug delivery system with Caco-2 cell model: Cremophor EL as the surfactant, Eur. J. Pharm. Sci. 91 (2016) 162–171. doi:10.1016/j.ejps.2016.06.011.
[34] J. Burgain, J. Scher, S. Lebeer, J. Vanderleyden, M. Corgneau, J. Guerin, C. Caillet, J.F.L. Duval, G. Francius, C. Gaiani, Impacts of pH-mediated EPS structure on probiotic bacterial pili–whey proteins interactions, Colloids Surf. B Biointerfaces. 134 (2015) 332–338. doi:10.1016/j.colsurfb.2015.06.068.
[35] Y.F. Dufrêne, Sticky microbes: forces in microbial cell adhesion, Trends Microbiol. 23 (2015) 376–382. doi:10.1016/j.tim.2015.01.011.
[36] G. Francius, D. Alsteens, V. Dupres, S. Lebeer, S. De Keersmaecker, J. Vanderleyden, H.J. Gruber, Y.F. Dufrêne, Stretching polysaccharides on live cells using single molecule force spectroscopy, Nat. Protoc. 4 (2009) 939–946. doi:10.1038/nprot.2009.65.
[37] A.P. Gunning, A.R. Kirby, C. Fuell, C. Pin, L.E. Tailford, N. Juge, Mining the "glycocode"--exploring the spatial distribution of glycans in gastrointestinal mucin using force spectroscopy, FASEB J. Off. Publ. Fed. Am. Soc. Exp. Biol. 27 (2013) 2342–2354. doi:10.1096/fj.12-221416.
[38] T.T. Le, T. Van de Wiele, T.N.H. Do, G. Debyser, K. Struijs, B. Devreese, K. Dewettinck, J. Van Camp, Stability of milk fat globule membrane proteins toward human enzymatic gastrointestinal digestion, J. Dairy Sci. 95 (2012) 2307–2318. doi:10.3168/jds.2011-4947.
[39] M.E. Sanders, M.L. Marco, Food formats for effective delivery of probiotics, Annu. Rev. Food Sci. Technol. 1 (2010) 65–85. doi:10.1146/annurev.food.080708.100743.
[40] M.L. Marco, S. Tachon, Environmental factors influencing the efficacy of probiotic bacteria, Curr. Opin. Biotechnol. 24 (2013) 207–213. doi:10.1016/j.copbio.2012.10.002.

559 [41] J. Wang, Z. Zhong, W. Zhang, Q. Bao, A. Wei, H. Meng, H. Zhang, Comparative analysis of
560 the gene expression profile of probiotic Lactobacillus casei Zhang with and without fermented
561 milk as a vehicle during transit in a simulated gastrointestinal tract, Res. Microbiol. 163
562 (2012) 357–365. doi:10.1016/j.resmic.2012.04.002.
563 [42] R. Würth, G. Hörmannsperger, J. Wilke, P. Foerst, D. Haller, U. Kulozik, Protective effect of
564 milk protein based microencapsulation on bacterial survival in simulated gastric juice versus
565 the murine gastrointestinal system, J. Funct. Foods. 15 (2015) 116–125.
566 doi:10.1016/j.jff.2015.02.046.
567 [43] T. Heidebach, P. Först, U. Kulozik, Microencapsulation of probiotic cells by means of rennet-
568 gelation of milk proteins, Food Hydrocoll. 23 (2009) 1670–1677.
569 doi:10.1016/j.foodhyd.2009.01.006.
570 [44] B. Lee, X. Yin, S.M. Griffey, M.L. Marco, Attenuation of Colitis by Lactobacillus casei BL23
571 Is Dependent on the Dairy Delivery Matrix, Appl. Environ. Microbiol. 81 (2015) 6425–6435.
572 doi:10.1128/AEM.01360-15.
573 [45] G. Deepika, R.A. Rastall, D. Charalampopoulos, Effect of food models and low-temperature
574 storage on the adhesion of Lactobacillus rhamnosus GG to Caco-2 cells, J. Agric. Food Chem.
575 59 (2011) 8661–8666. doi:10.1021/jf2018287.
576

577

578 Figure 1

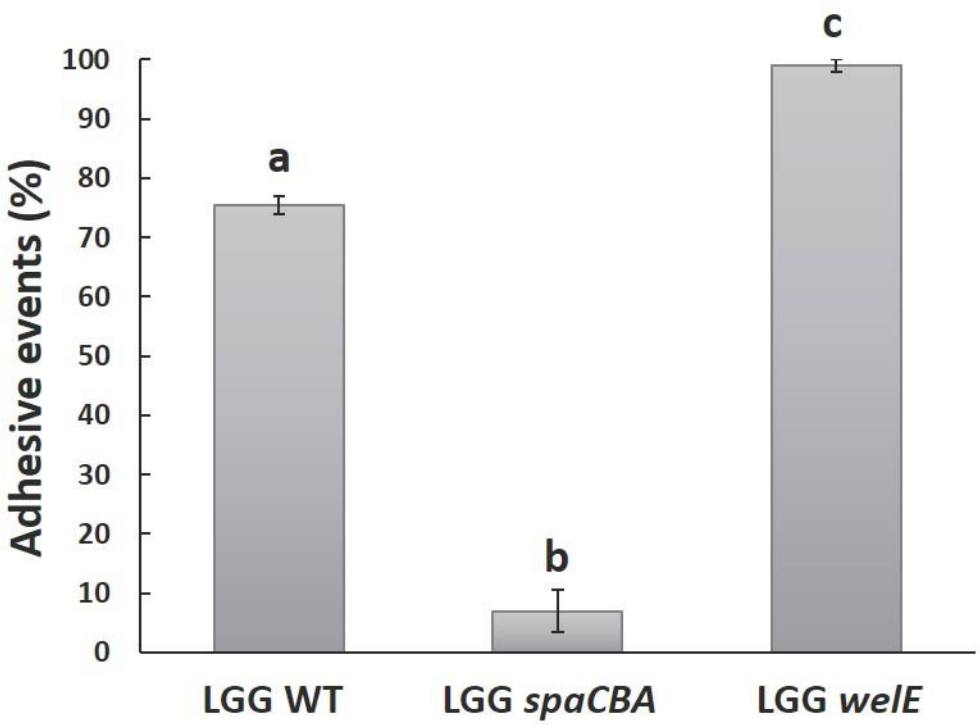

579

580

581 Figure 2

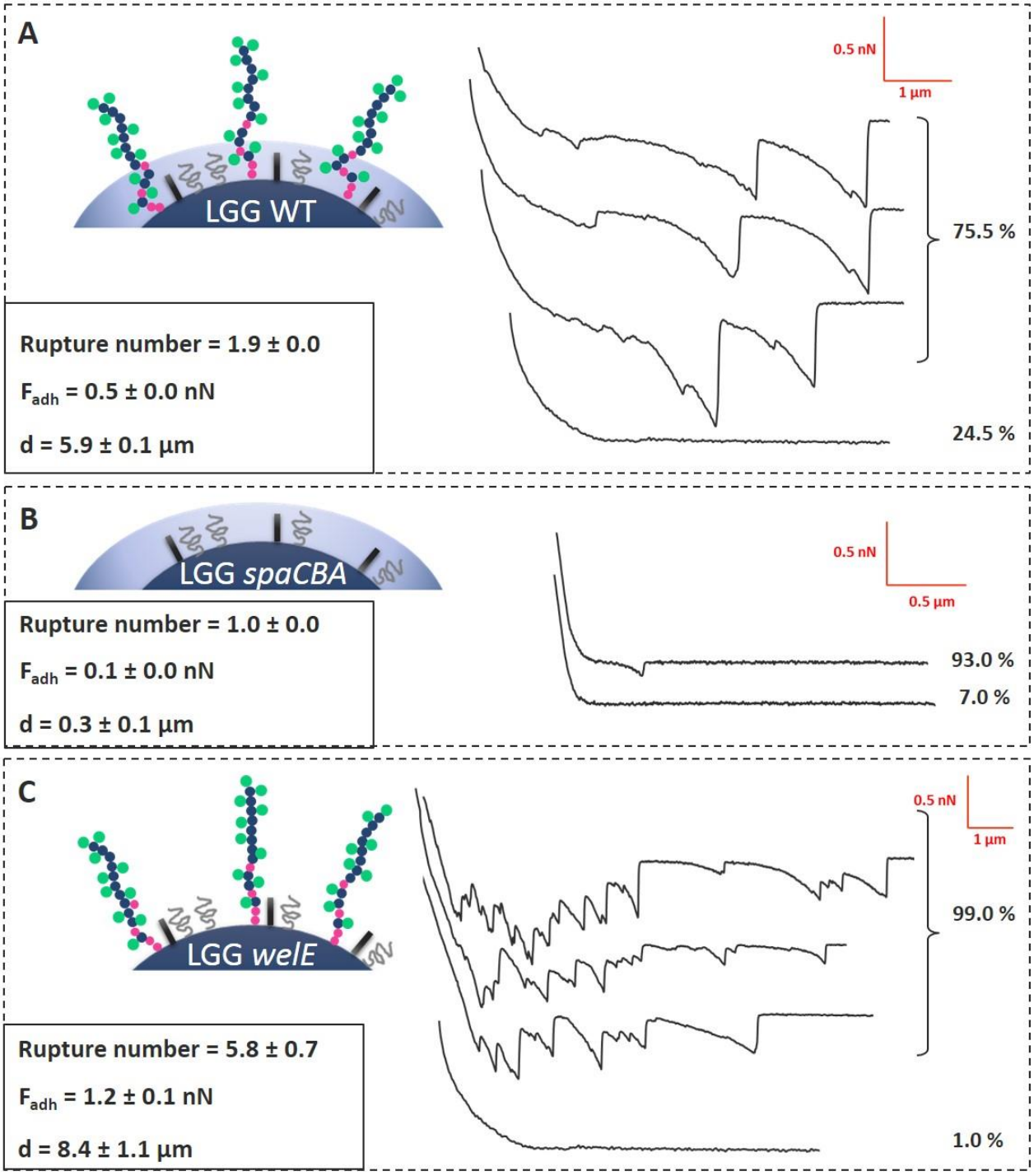

582

583

584 Figure 3

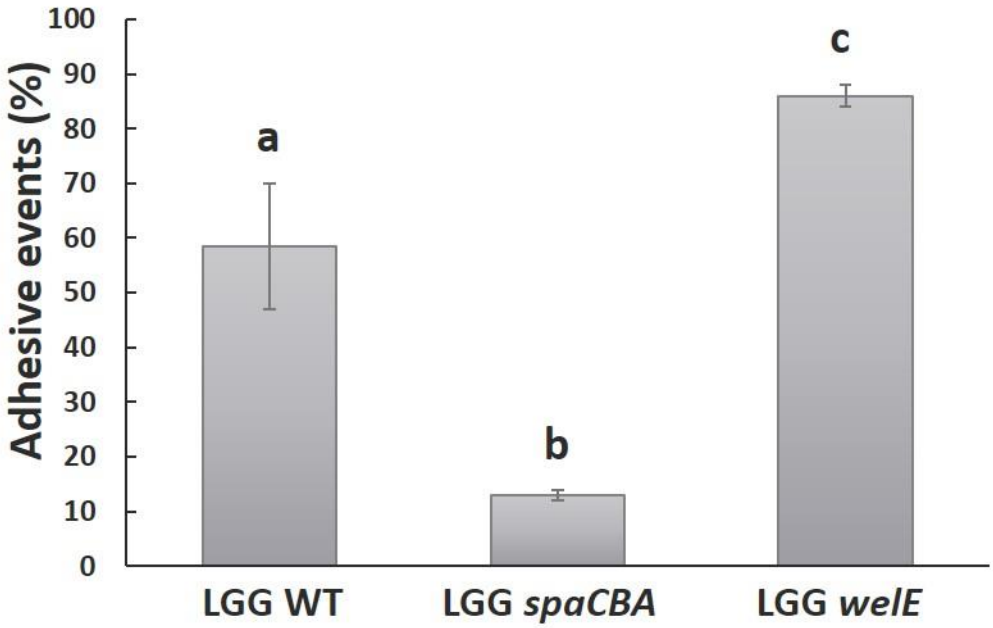

585

586

587 Figure 4

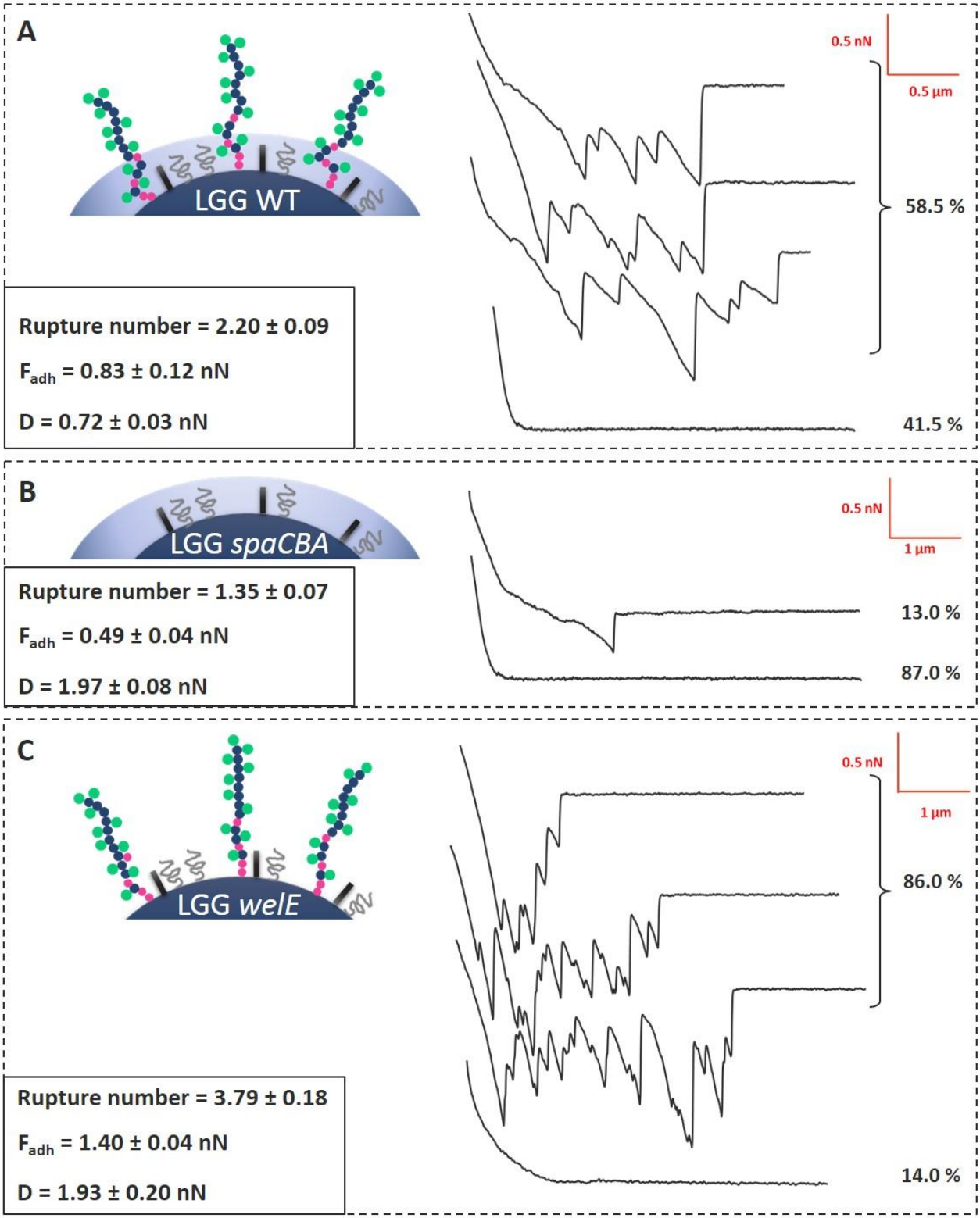

588

589 Figure 5

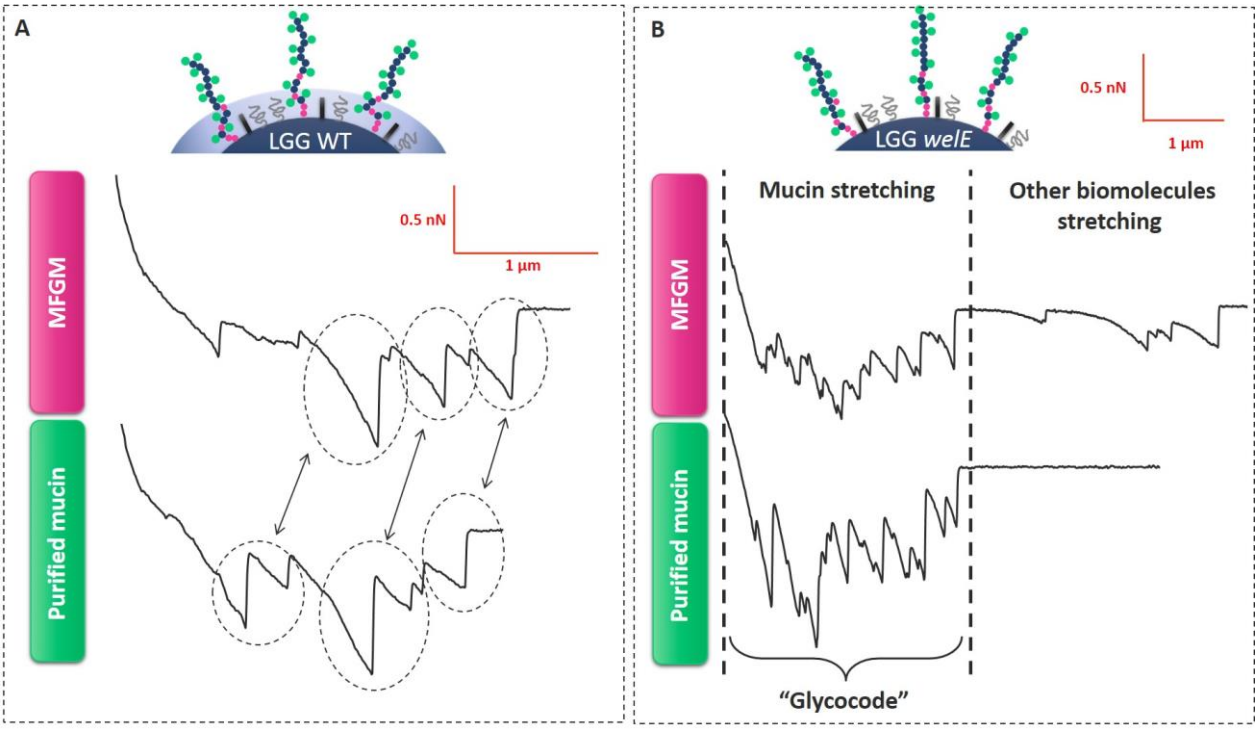

590

591

592 Figure 6

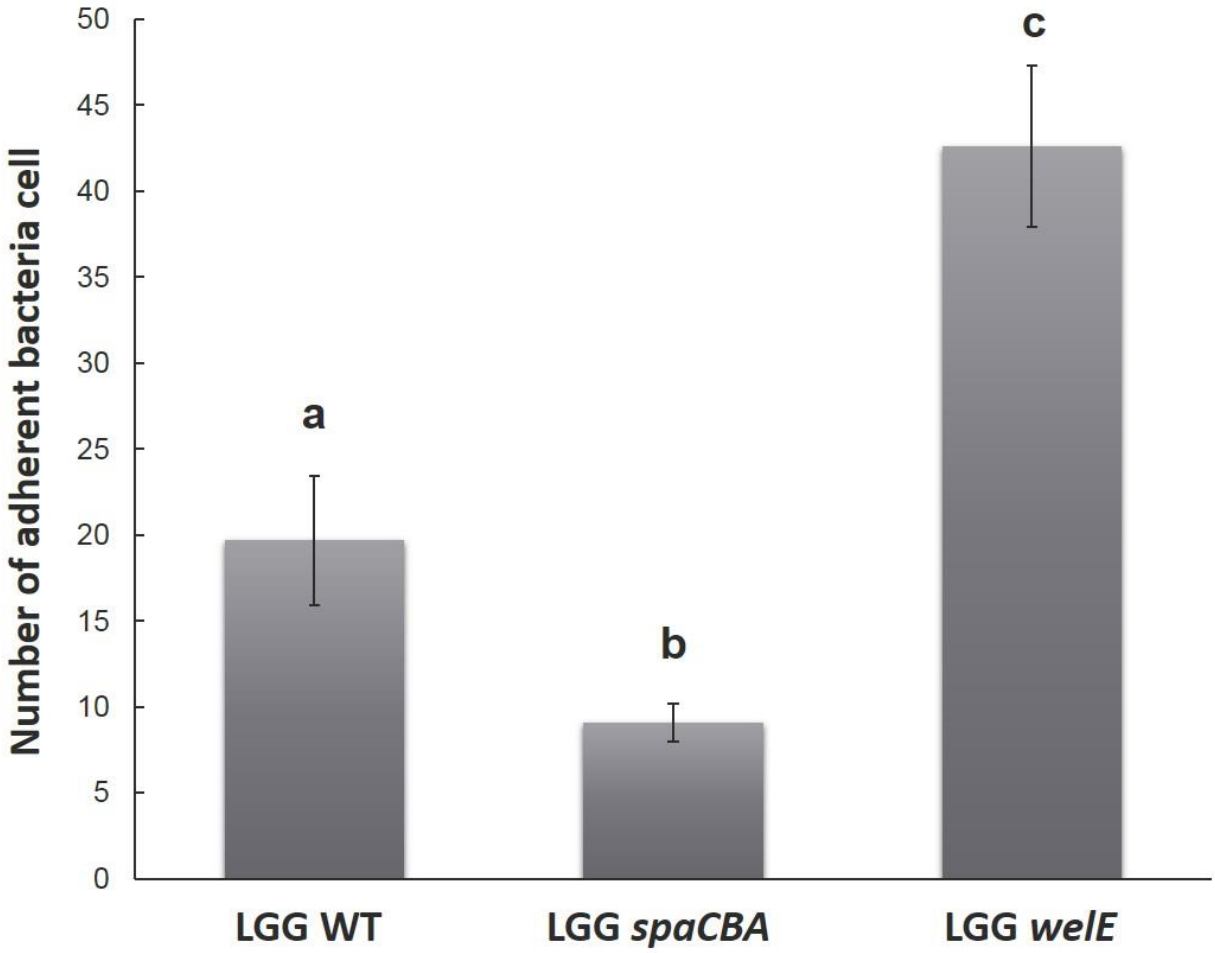

593

594

595 Figure 7

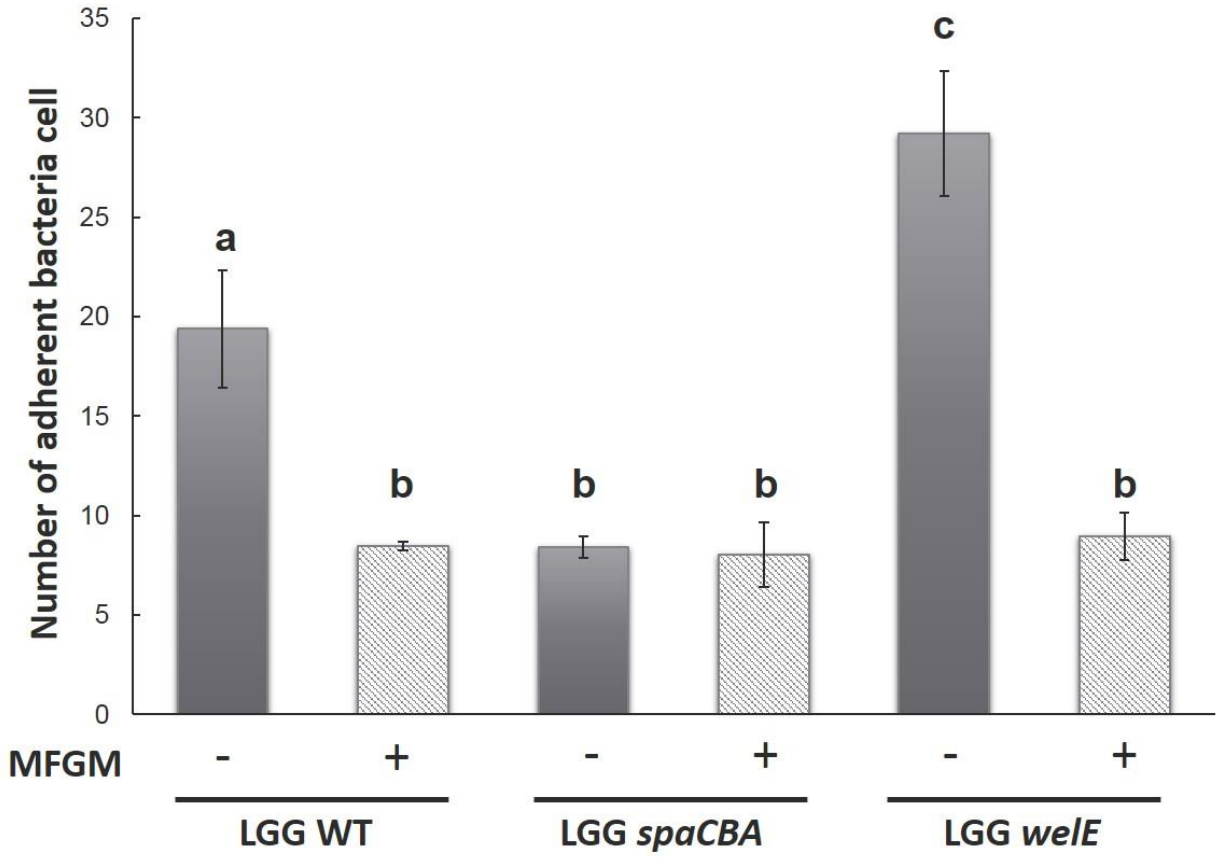

596

597

598 Figure 8

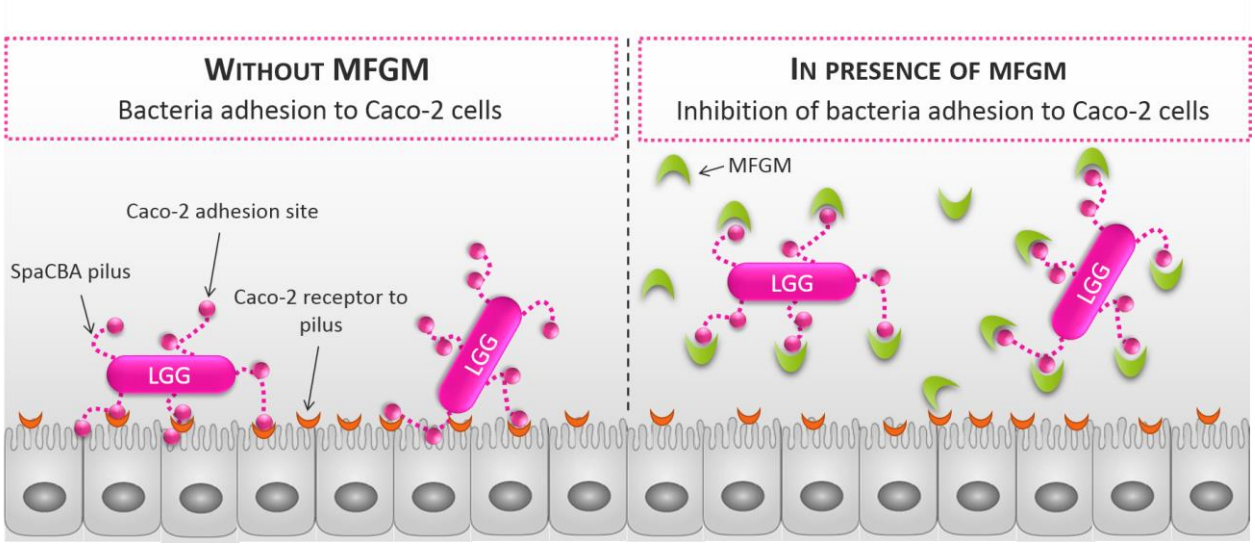

599

600

601 ToC

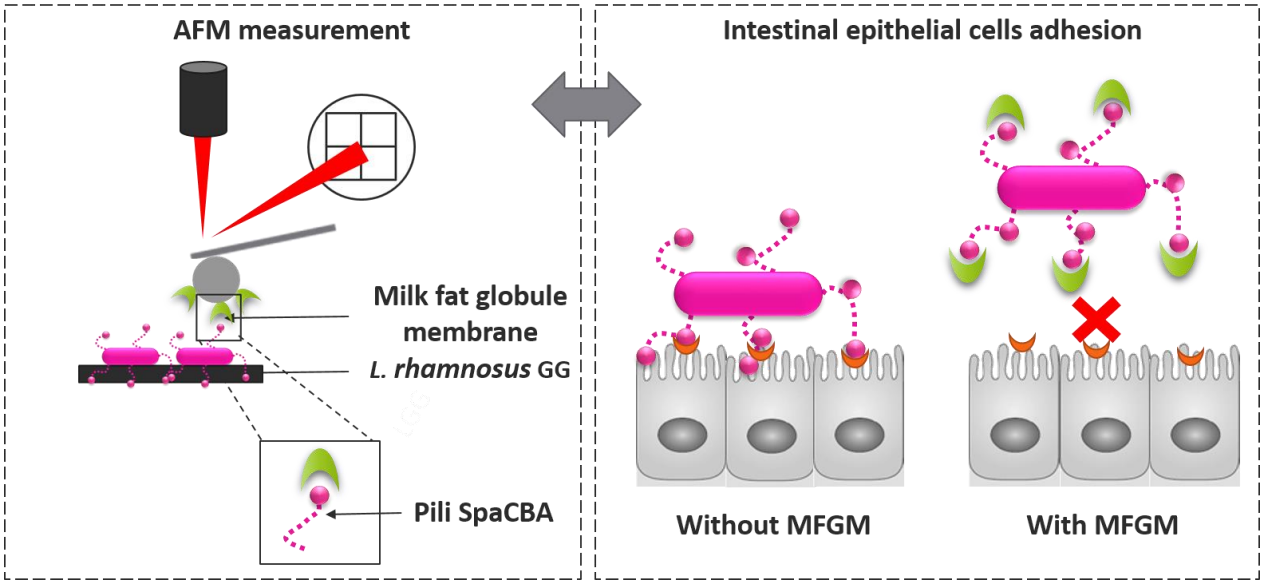

602

603

Figure captions

Figure 1: Adhesive events quantification between MFGM and LGG WT and two surface mutants (LGG *spaCBA* mutant and LGG *welE* mutant). Means ± SEM followed by a different superscript letter indicate a significant difference ($P<0.05$)

Figure 2: Adhesion between MFGM AFM probes and LGG WT, LGG *spaCBA*, and LGG *welE* surface mutants. Representative retraction curves observed between MFGM and LGG WT (A), LGG *spaCBA* (B) and LGG *welE* (C) are presented. F_{adh}: maximal rupture force; d: maximal distance of rupture

Figure 3: Adhesive events quantification between purified mucin and LGG WT, LGG *spaCBA* mutant, and LGG *welE* mutant urface mutants. Means ± SEM followed by a different superscript letter indicate a significant difference ($P<0.05$)

Figure 4: Adhesion between purified mucin and LGG WT and LGG *spaCBA* and LGG *welE* surface mutants. Representative retraction curves observed between mucin AFM probes and LGG WT (A), LGG *spaCBA* (B) or LGG *welE* (C) are presented. F_{adh}: maximal rupture force; d: maximal distance of rupture

Figure 5 : Representative retraction curves observed during adhesion between LGG WT (A) or LGG *welE* (B) and purified mucin; comparison with representative retraction curves recorded with MFGM

Figure 6: Adhesion of LGG WT and its derivative mutants (LGG *spaCBA* and LGG *welE*) to a Caco-2 TC7 cell line after 2 h of co-incubation. Data represent means ± SEM from at least two independent experiments performed with each strain in triplicate (n = 2 × 3). Means ± SEM followed by a different superscript letter indicate a significant difference ($P<0.05$)

Figure 7: Impact of MFGM addition on the adhesion of LGG WT and its derivative mutants (LGG *spaCBA* and LGG *welE* mutant) to a Caco-2 TC7 cell line. The symbols "+" and "-" mean the presence or the absence of MFGM during the adhesion, respectively. Data represent means ± SEM from at least two independent experiments performed with each strain in triplicate (n = 2 × 3). Means ± SEM followed by a different superscript letter indicate a significant difference ($P > 0.05$)

Figure 8: Mechanism proposed for the inhibition of the adhesion phenomenon between LGG and Caco-2 TC7 cells in presence of MFGM